Memorias del Congreso Nacional de Control Automático 2012
Cd. del Carmen, Campeche, México, 17 al 19 de Octubre de 2012

Virtual Serial Power Split Strategy for Parallel Hybrid Electric Vehicles

Alfonso Pantoja-Vazquez[1], Guillermo Becerra[2], Luis Alvarez-Icaza[3]
Instituto de Ingeniería - Universidad Nacional Autónoma de México
Coyoacán, D.F. 04510, México

***Abstract*— A new strategy for hybrid electric vehicles power flow control is presented. The strategy takes advantage of the kinematic and dynamic constraints of a planetary gear system used to couple the internal combustion engine and the electric machine. The strategy is able, most of the time, to operate the internal combustion engine at maximum efficiency and to keep the battery state of charge on a desired level by making use of an easy to tune PI controller. The computational requirements of the strategy are low. Although the strategy is not formally proven optimal, it is inspired on optimal control theory.**

I. INTRODUCTION

Concern on the use of fossil fuels is an important matter for today's society since they are a nonrenewable resource and because of global warming and its socio-economical impacts. The reduction of energy consumption on human transportation has been a challenge for governments, industry and researchers on the last years (Gong *et al.*, 2008; Schouten *et al.*, 2002).

Hybrid Electric Vehicles (HEV) are an option to help solving these problems. They use a combination of two or more power sources, usually an Internal Combustion Engine (ICE) and an Electric Machine (EM). HEV can reduce energy consumption and pollutant emissions compared to conventional vehicles due to the extra degree of freedom added by the EM, and also due to the ability of regenerative braking. All of these benefits are available, without sacrificing vehicle's conventional attributes like performance, safety and reliability. These benefits also imply that the performance of Hybrid Electric Vehicles (HEV) is strongly related to the power split strategy (Lin *et al.*, 2003; Musardo *et al.*, 2005; Sciarretta *et al.*, 2004).

In the literature several design approacachieves hes have been proposed for power split strategies. Some of them based on heuristics approaches, like fuzzy logic, (Langari and Won, 2003; Schouten *et al.*, 2002), fuzzy logic tunned with genetic algorithms (Zhang *et al.*, 1997) and rule based strategies optimized with Dynamic Programming (DP) (Lin *et al.*, 2002; Lin *et al.*, 2003). Approaches based on optimal control theory can be found, for example in (Delprat *et al.*, 2001; Delprat *et al.*, 2004; Kessels *et al.*, 2008). The Equivalent Consumption Minimization Strategy (ECMS) is presented in (Sciarretta *et al.*, 2004; Zhang *et al.*, 2010) and a predictive control is described in (Borhan *et al.*, 2009). There are also approaches based on DP or that use DP to tune the proposed strategy (Johannesson and Egardt, 2008; Lin *et al.*, 2003; van Keulen *et al.*, 2010). More recently, a new strategy has been proposed in (Becerra *et al.*, 2011) for parallel HEVs. This strategy takes advantage of the kinematic and dynamic constraints from a Planetary Gear System (PGS) used as the mechanical coupling between the ICE and the EM. These constraints give one more degree of freedom from the power split strategy point of view.

Although DP yields an optimal solution, it is not suitable for online implementation because of the dependence on the future driving conditions and due to very high computational requirements. On the other hand, strategies based on ECMS are easier to implement, but their performance may vary depending on the driving cycle and on its tunning parameters, which are not always easy to tune, (Zhang *et al.*, 2010; Sciarretta and Guzzella, 2007). Rule based strategies are the strategies most used for production vehicles since they are easy to implement, but its performance is very poor since the optimization is based on static preoptimized maps, moreover, it depends on the driving cycle and the battery charge level is not guaranteed (Sciarretta and Guzzella, 2007). The strategy presented on this work has the advantages of being easy to implement and low computational requirements. The ICE performance is preoptimized offline with a static map and the battery charge level is guaranteed with a PI compensator. Even when it is not formally proven to be optimal, this strategy is inspired in optimal control theory.

Similar to the strategy presented in (Becerra *et al.*, 2011), the present work takes advantage of the PGS as the mechanical coupling device between the ICE and the EM. Using the kinematic constraint on the PSG, the ICE power is kept on its most efficient operation point almost all the time and the EM receives the excess or delivers the lack of power in order to satisfy the power required in the driving cycle. By itself, this strategy tends to deplete or fill in the battery, depending on the driving cycle, to avoid this, a PI controller is added to adjust the ICE power when the battery State Of Charge (SOC) is different to a reference.

The rest of this paper is organized as follows. In the second section, the model and configuration used for simulations of the HEV are presented; in the third section, the problem is formulated and the *virtual serial strategy*

[1] apantojav@iingen.unam.com
[2] gbecerran@iingen.unam.com
[3] alvar@pumas.iingen.unam.mx

is presented; simulation results of the proposed strategy over several driving cycles and its parameter robustness is analyzed in the fourth section; finally, conclusions and future work are presented in the fifth section.

II. HYBRID VEHICLE MODEL

The HEV configuration selected in this work is a parallel one, where the ICE and the EM are coupled via a PGS, see Fig. 1, as proposed in (Becerra *et al.*, 2011).

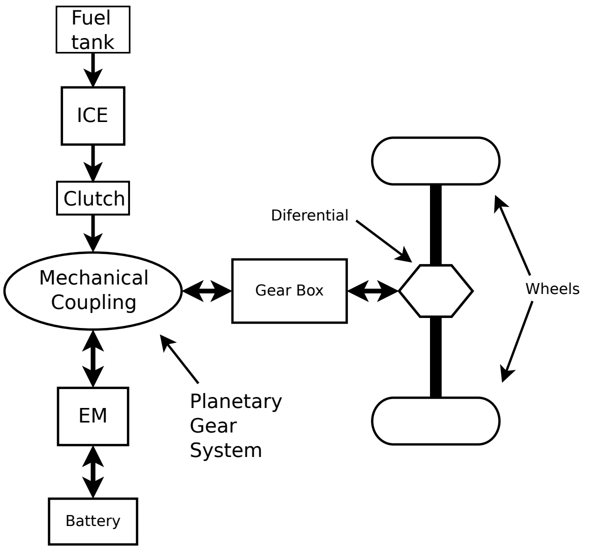

Fig. 1. Parallel HEV configuration.

A. Vehicle Model

The power requested by the power train P_p is calculated by modeling the vehicle like a moving mass subject to a traction force F_{tr}, provided by the power sources (Lin *et al.*, 2003). The vehicle velocity dynamic $v(t)$ is

$$m\frac{dv(t)}{dt} = F_{tr} - \frac{1}{2}\rho_a C_d A_d v(t)^2 - mgC_r\cos(\gamma(t)) -mg\sin(\gamma(t)) \quad (1)$$

where ρ_a is the air density, C_d is the aerodynamic drag coefficient, A_d is the vehicle frontal area, m is the vehicle mass including the cargo mass, g is the gravity acceleration constant, C_r is the tire rolling resistance coefficient and $\gamma(t)$ is the road slope.

The torque and speed demanded by the power train, τ_p and ω_p, are respectively

$$\omega_p = \frac{R_f}{R_w}R(t)v(t) \quad (2)$$

$$\tau_p = \frac{R_w}{R_f}\frac{1}{R(t)}F_{tr} \quad (3)$$

where $R(t)$ is the gearbox ratio, R_f is the final drive ratio and R_w is the wheel radius.

Finally, the power at the power train is

$$P_p(t) = \omega_p(t)\tau_p(t) = v(t)F_{tr}(t) + P_{acc} \quad (4)$$

where P_{acc} is the power required by the vehicle accessories.

B. ICE Model

The ICE is modeled through a static nonlinear map, taken from ADVISOR (Markel *et al.*, 2002), which relates the ICE fuel rate consumption $\dot{m}_f$, with the torque at the crankshaft τ_{ice} and the engine speed ω_{ice}, in other words

$$\dot{m}_f = f(\omega_{ice}, \tau_{ice}) \quad (5)$$

Using the fuel Lower Heat Value, the ICE efficiency map is generated, Fig. 2 shows the map for the ICE used in this work. From this point of view, when the ICE is operating, it is desirable to operate it on the most efficient points of the map.

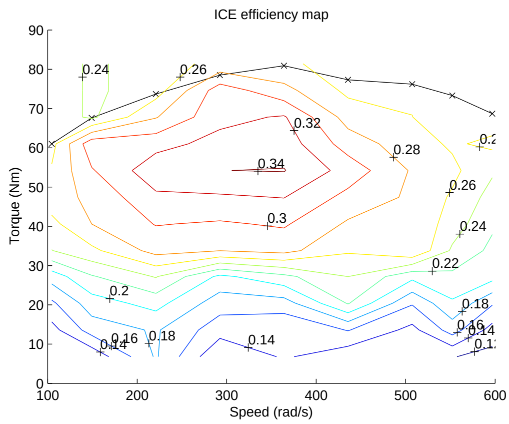

Fig. 2. ICE efficiency map.

C. EM Model

In an HEV, the EM can work as motor or as generator depending if it is required to give or receive energy. EM is modeled also using a static nonlinear map which relates the EM speed ω_{em} and EM torque τ_{em} with an efficiency when it works as generator η_{gen}, and another one when it works as motor η_{mot}.

In other words, if the EM works as motor, $\tau_{em} \geq 0$, then

$$P_{em} = \eta_{mot}(\tau_{em}, \omega_{em})P_{bat} \quad (6)$$

or if it works as generator, $\tau_{em} < 0$, then

$$P_{bat} = \eta_{gen}(\tau_{em}, \omega_{em})P_{em} \quad (7)$$

with $P_{em} = \tau_{em}\omega_{em}$ and P_{bat} is the electric power.

D. Battery

The battery is modeled like a voltage source v_{oc} with an internal resistance R_{int} which depends on the SOC (Lin *et al.*, 2003). The equivalent circuit is shown in Fig. 3, where v_{oc} is the battery's open circuit voltage, i_{bat} is the bus current and v_{bat} is the bus voltage.

Using the Kirchoff's voltage law, i_{bat} is found by solving

$$R_{int}(SOC)i_{bat}^2 - v_{oc}i_{bat} + P_{bat} = 0 \quad (8)$$

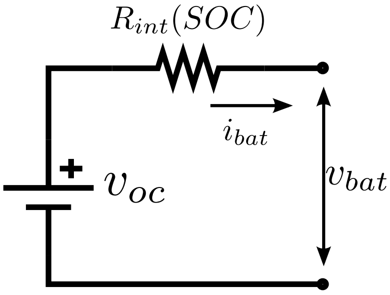

Fig. 3. Battery equivalent circuit.

and v_{bat} is

$$v_{bat} = v_{oc} - R_{int}(SOC)i_{bat} \tag{9}$$

Finally, the SOC is obtained from the expression

$$SOC(t) = min\left\{1, max\left\{0, \frac{Q_0 - \int_{t_0}^{t} i_{bat}(\tau)d\tau}{Q_T}\right\}\right\} \tag{10}$$

where Q_0 is the initial charge and Q_T is the total charge the battery can store.

E. Planetary Gear System

A PGS is used as the mechanical coupling between the ICE and the EM, as proposed in (Becerra *et al.*, 2011). A schematic is shown in Fig. 4. On this coupling, the ICE output shaft is connected to the sun gear, the EM to the ring gear and the gear box is connected to the carrier shaft.

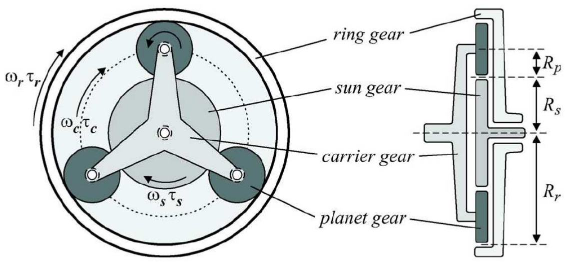

Fig. 4. Planetary Gear System.

With $k = R_r/R_s$, the angular speeds on the PGS satisfy

$$\omega_c = \frac{1}{k+1}\omega_s + \frac{k}{k+1}\omega_r \tag{11}$$

and the balance of power satisfies

$$\tau_c\omega_c = \tau_s\omega_s + \tau_r\omega_r \tag{12}$$

where ω is angular speed, τ is torque and subscripts s, c and r refer to sun gear, planet carrier and ring gear, respectively.

III. POWER SPLIT STRATEGY

The problem to be solved, from the optimization point of view, is to minimize the fuel consumption over a desired driving cycle

$$\min J = \int_0^{t_c} \dot{m}_f(\omega_{ice}(t), \tau_{ice}(t))dt \tag{13}$$

subject to

$$\omega_{ice\,\min} \leq \omega_{ice}(t) \leq \omega_{ice\,\max} \tag{14}$$
$$\tau_{ice\,\min} \leq \tau_{ice}(t) \leq \tau_{ice\,\max} \tag{15}$$
$$\omega_{em\,\min} \leq \omega_{em}(t) \leq \omega_{em\,\max} \tag{16}$$
$$\tau_{em\,\min} \leq \tau_{em}(t) \leq \tau_{em\,\max} \tag{17}$$
$$P_{bat\,\min} \leq P_{bat} \leq P_{bat\,\max} \tag{18}$$
$$SOC_{\min} \leq SOC(t) \leq SOC_{max} \tag{19}$$

where subscripts $\min$ and $\max$ means the minimum and maximum value for the constrained variable and t_c is the duration of the driving cycle.

When the ICE is used, a feasible solution would be to only operate the ICE in the regions where it spends less fuel per power generated, i.e., in the most efficient operation points like in a serial HEV configuration. The strategy proposed in this work is based on this solution.

In addition to keep the ICE on its most efficient region when it is used, the vehicle must follow the driving cycle. In consequence, the problem to be solved is to meet the power P_p on the output of the PGS, while the ICE operates on its most efficient region. This problem, of providing the power P_p, has multiple solutions, since many combinations of torque and speed at each power source can yield the demanded power P_p.

Rewriting Eq. (11) and (12) in terms of the ICE and EM variables, the equations that constraint the solution of this problem are

$$P_p = \tau_p\omega_p = \tau_{ice}\omega_{ice} + \tau_{em}\omega_{em} = P_{em} + P_{ice} \tag{20}$$
$$\omega_p = \frac{1}{k+1}\omega_{ice} + \frac{k}{k+1}\omega_{em} \tag{21}$$

where the ICE is associated with the sun gear, the EM with the ring gear and the driving wheels with the carrier.

The approach presented on this work is based on the following assumptions:

1) The strategy meets the required power to perform the driving cycle, if it is feasible.
2) The ICE operation is optimized in order to operate it on its highest efficient power and speed, while possible.
3) The EM is used to generate or absorb the lack or excess of power, once the ICE power has been set.
4) A PI controller adjusts dynamically the use of the ICE in order to keep the SOC near a given reference.

A block diagram of the proposed strategy is shown in Fig. 5.

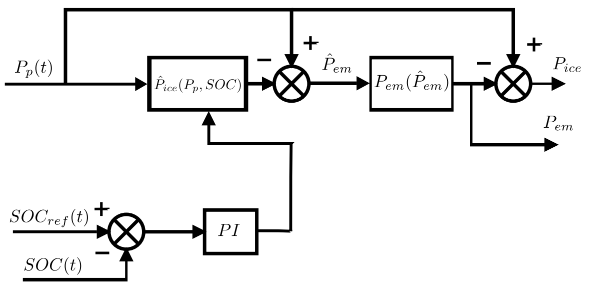

Fig. 5. Strategy Topology.

A. ICE Power

When $P_p > 0$, the first step of this strategy is to determine a pre-value for the ICE power $\hat{P}_{ice}$, the final P_{ice} will be set at the end to assure tracking of the driving cycle. In most of the cases $\hat{P}_{ice}$ will be the final power.

There are two cases when the ICE should operate out of its maximum efficiency operation point $ICE_{eff\,\max}$, and they are:

1) When the required driving cycle power is very low or very high, the ICE should be off or should complement the lack of power, respectively.
2) When the SOC is not on the given reference, the ICE has to compensate this excess or lack of power.

A bang-bang type solution would be to saturate the ICE when the previous cases occurs, but instead, like in (Becerra *et al.*, 2011), a soft curve is proposed based on the previous observations. The curve depends on the required power and on the SOC

$$\hat{P}_{ice}(\hat{P}_p, SOC) = \alpha(\hat{P}_p, SOC) P_{ice\,\max} \tag{22}$$

where $\hat{P}_p$ is the normalized value of P_p defined as $\hat{P}_p = \frac{P_p}{P_{ice\,\max}}$ and $\alpha(\hat{P}_p, SOC) \in [0, 1]$, defined as

$$\alpha(\hat{P}_p, SOC) = \frac{\left(2\hat{P}_p + \xi + SOC_{comp}(SOC) - 1\right)^7}{2} + \frac{P_{ice\_eff}}{P_{ice\,\max}} \tag{23}$$

which ranges between 0 and 1. P_{ice_eff} is the ICE most efficient power and $P_{ice\,\max}$ is the ICE maximum power. $\xi \in [0, 1]$ assures that $\alpha(\hat{P}_p, SOC) = 1$ when $P_p = P_{ice\,\max}$ (or $\hat{P}_p = 1$) and $SOC_{comp} = 0$. For a given P_{ice_eff} and $P_{ice\,\max}$, ξ is defined as

$$\xi = \sqrt[7]{2(1 - \frac{P_{ice\_eff}}{P_{ice\,\max}})} - 1 \tag{24}$$

$SOC_{comp} \in [-1, 1]$ is the SOC compensator for the P_{ice}. Its role is to move the power calculated in Eq. (23) according to the difference between a reference for the SOC, SOC_{ref}, and the instantaneous SOC, $SOC(t)$. In other words, if $SOC(t)$ is below to SOC_{ref}, more use of the ICE is expected, and if $SOC(t)$ is over SOC_{ref}, less use of the ICE is expected.

Based on the efficiency map, Eq. (23) was designed in order to operate the ICE on its most efficient power, P_{ice_eff}, as much as possible. It could be appreciated on Fig. 6, which shows the plot of $\alpha(\hat{P}_p, SOC)$ with $\frac{P_{ice\_eff}}{P_{ice\,\max}} = 0.5$ and $SOC_{comp} = 0$.

Fig. 7 shows the plot of $\alpha(\hat{P}_p, SOC)$ with several values of SOC_{comp}. It can be seen that, to keep $SOC(t)$ over a desired SOC_{ref}, positive values of SOC_{comp} are expected when $SOC(t)$ is below SOC_{ref}, and negative values of SOC_{comp} are expected when $SOC(t)$ is over SOC_{ref}.

To achieve this behavior of SOC_{comp}, a PI controller is used in order to keep the SOC around a given reference. This controller is necessary because without it the strategy tends to fill up or to deplete the battery, depending on the driving cycle. The SOC compensator SOC_{comp} is defined as follows

$$SOC_{comp}(SOC) = k_p \left(SOC_{ref} - SOC(t)\right) + k_i \int_0^t \left(SOC_{ref} - SOC(\tau)\right) d\tau \tag{25}$$

where k_i and k_p are the tunning parameters for the PI controller.

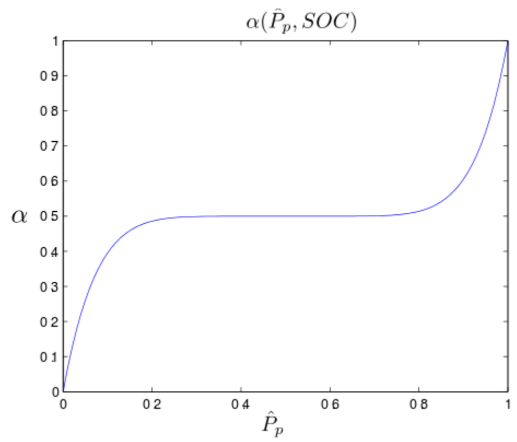

Fig. 6. Plot of $\alpha(\hat{P}_p, SOC)$.

At this point, a first proposal for the ICE power could be calculated, but the final P_{ice} is calculated after the EM power is set, to assure meeting the requested power, as illustrated in Fig. 5. Setting of EM power is explained later on. The final value for P_{ice} is

$$P_{ice} = \max\left(\hat{P}_{ice}, P_p - P_{em}\right) \tag{26}$$

which is saturated between 0 and $P_{ice\,\max}$.

When P_{ice} has been set, ω_{ice} and τ_{ice} need to be determined. Taking advantage of the kinematic relation of the PGS, expressed in Eq. (20), ω_{ice} can be set to achieve the maximum efficiency for the ICE at a given power. The algorithm presented in the Appendix is used for this purpose, it is solved offline and stored. Finally, the ICE

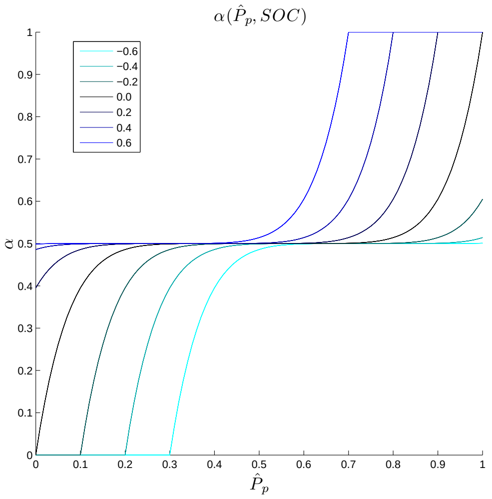

Fig. 7. Plot of $\alpha(\hat{P}_p, SOC)$ for severals values of SOC_{comp}.

torque is set with

$$\tau_{ice} = \begin{cases} 0 & \text{for } \omega_{ice} = 0 \\ \dfrac{P_{ice}}{\omega_{ice}} & \text{for } \omega_{ice} > 0 \end{cases} \tag{27}$$

B. EM Power

It is expected that the EM compensates the difference between P_p and P_{ice} in order to meet the required power, although it is limited by the EM maximum and minimum power $P_{em\,\max}$ and $P_{em\,\min}$. As it is shown in Fig. 5, a pre-value for the EM power is

$$\hat{P}_{em} = P_p - \hat{P}_{ice} \tag{28}$$

and the final value for the EM power is

$$P_{em}(\hat{P}_{em}) = \max\left(P_{em\,\min}, \min\left(P_{em\,\max}, \hat{P}_{em}\right)\right) \tag{29}$$

Finally, from Eq. (20), EM speed and torque are calculated

$$\omega_{em} = \frac{k+1}{k}\left(\omega_p - \frac{\omega_{ice}}{k+1}\right) \tag{30}$$

$$\tau_{em} = \begin{cases} 0 & \text{for } \omega_{em} = 0 \\ \dfrac{P_{em}}{\omega_{em}} & \text{for } \omega_{em} \neq 0 \end{cases} \tag{31}$$

C. Regenerative Braking

In case of braking $P_p < 0$, it is necessary to recover as much energy as possible, taking care of not damaging the batteries (Becerra *et al.*, 2011). In this case $P_{ice} = 0$ and P_{em} is

$$P_{em}(SOC) = \max(P_p, \beta(SOC) P_{em\,\max}) \tag{32}$$

with

$$\beta(SOC) = 0.5\left[\tanh(A_1(SOC - SOC_{\max}))\right] - 0.5 \tag{33}$$

where A_1 is a design parameter. Fig. 8 shows the plot of β for $A_1 = 0.8$ and $SOC_{\max} = 90\%$.

Finally, the required power at friction brakes is

$$P_f = P_p - P_{em} \tag{34}$$

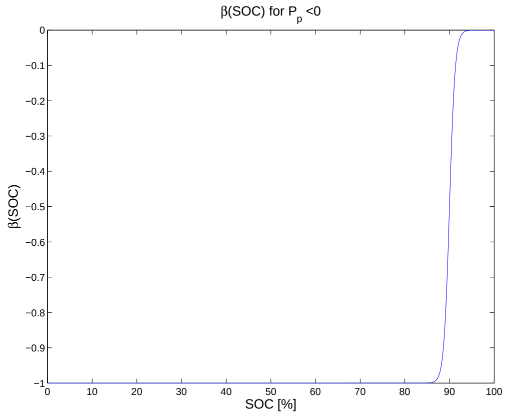

Fig. 8. Regenerative braking power in function of SOC.

IV. SIMULATION RESULTS

On this section, results of simulating on ADVISOR (Markel *et al.*, 2002; Gao *et al.*, 2007) the vehicle and the strategy presented on the previous sections are shown. To get an idea of the strategy performance, it is compared against a rule based strategy, available in ADVISOR, with the same vehicle parameters but with a normal parallel configuration, it is the ICE and the EM connected through a gear with a different ratio each one. Main parameters for the simulated vehicle are shown in Table I.

Total mass	912 kg
ICE peak power	41 kW
Li-Ion Battery (6 Ah and $V_{nom} = 267V$) peak power	25 kW
EM power peak power	25 kW
Gear box	5 speeds

TABLE I

MAIN PARAMETERS FOR THE SIMULATED VEHICLE.

Strategy parameters are shown in Table II. ICE_{map} was taken from the ADVISOR database.

SOC_{ref}	70%
$SOC_{\max}$	85 %
A_1	1
k (PGS ratio)	5
P_{ice_eff}	20kW
$P_{ice\,\max}$	41kW
k_p	1
k_i	0.01

TABLE II

POWER SPLIT STRATEGY PARAMETERS.

Table III shows the fuel consumption for the proposed strategy for two driving cycles, and simulation are shown in Figs. 9 and 10. Table IV shows the fuel consumption for the same driving cycles when a rules based strategy is used and simulation results for this rules based strategy are shown in Figs. 11 and 12.

It is convenient to emphasize that initial SOC on simulations where set, after several trials, to coincide with the final SOC. Taking this in consideration, the fuel consumption is only due to the power split strategy used to move the vehicle and not affected by the electrical energy in the storage system and gives a clear picture about the strategy performance. It is evident that there is a great improvement with the proposed strategy, specially on urban conditions.

Cycle	Initial SOC (%)	Final SOC (%)	Fuel Consumption (L/100 km)
UDDS	71.14	71.14	4.2996
HWFET	70.72	70.72	4.3169

TABLE III

SIMULATION RESULTS FOR THE VIRTUAL SERIAL STRATEGY.

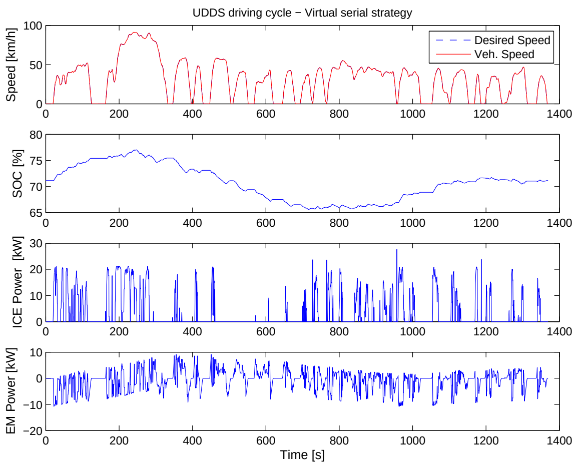

Fig. 9. Virtual Serial Strategy over UDDS cycle simulation results.

Cycle	Initial SOC (%)	Final SOC (%)	Fuel Consumption (L/100 km)
UDDS	69.66	69.66	6.5246
HWFET	71.5	71.5	4.8696

TABLE IV

SIMULATION RESULTS FOR THE RULES BASED STRATEGY.

In Figs. 9 and 10 it can be appreciated that the ICE works always around its more efficient power, 19.7kW. This is confirmed in Figs. 13 and 14, that shows ICE efficiency histograms ($P_ice > 0$) for UDDS and HWFET cycles.

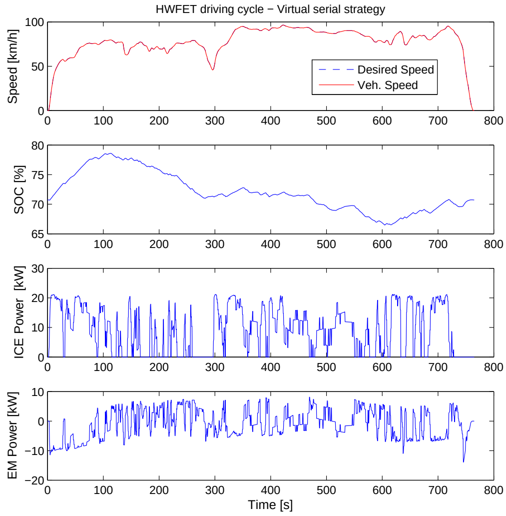

Fig. 10. Virtual Serial Strategy over HWFET cycle simulation results.

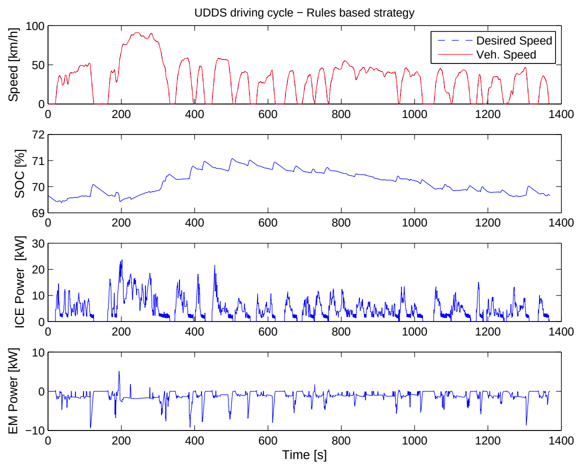

Fig. 11. Rules based strategy over UDDS cycle simulation results.

V. CONCLUSIONS

In this work a new strategy for HEV power flow control has been proposed. It is supported by an innovative way to couple the power sources presented in (Becerra *et al.*, 2011). Although It is not proven to be optimal, it is inspired on optimal control theory. An offline procedure was designed to optimize the ICE speed given a ICE power. The proposed strategy has the advantage of being easy to implement as it has low computational requirements, compared with other power split approaches.

The strategy operates the ICE on its most efficient region most of the time and a PI controller is used to compensate the deviation of the SOC. This compensator has the advantage of being easy to tune since, it depends only in two parameters. Although in this work a PI controller was used, other controllers could be used.

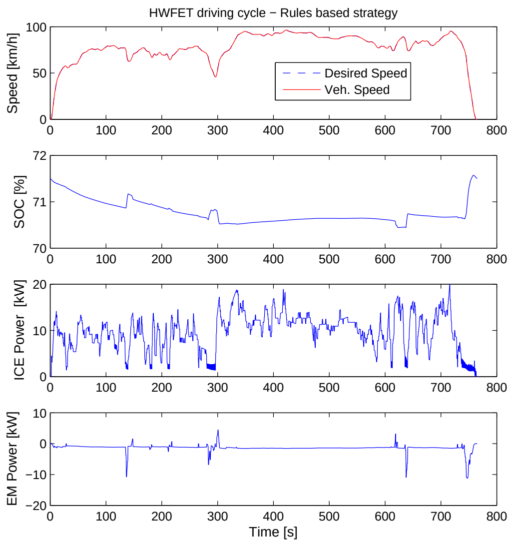

Fig. 12. Rules based strategy over HWFET cycle simulation results.

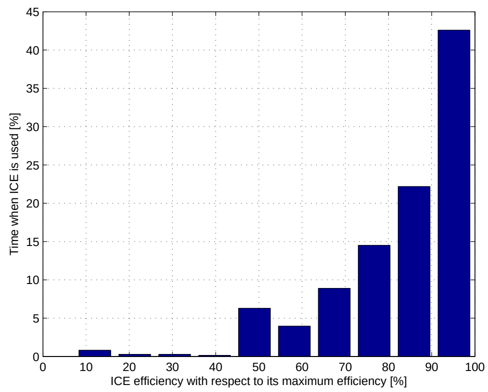

Fig. 13. ICE efficiency histogram when ICE is used in cycle UDDS.

Simulation results show a better performance of the strategy compared with a rules based strategy. They also show that, effectively, the ICE operates around its most efficient region. Results demonstrate also that the strategy is robust, from the driving cycle point of view, since it shows good performance for urban conditions as for highway conditions.

A. Future Work

There are several topics that are open on this work:

1) Formally proving the conditions for the optimality of the strategy.
2) Comparing the strategy with the DP solution as a way to evaluate its performance.
3) Studying the effect of having *a priori* information of the driving cycle on the performance of the strategy.

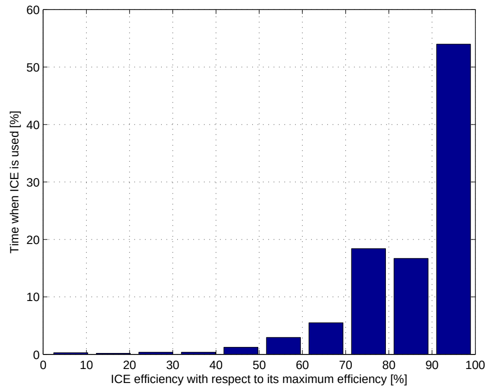

Fig. 14. ICE efficiency histogram when ICE is used in cycle HWFET.

4) Studying the effect of the strategy on the dimensioning of the HEV power sources (ICE, EM and battery).
5) Testing the performance of the strategy with other controllers for the SOC compensator instead of the PI controller.

APPENDIX

ICE Speed Optimization: In this section an algorithm to find the most efficient ICE speed, for a given power, using an efficiency map is presented.

Once P_{ice} has been set, it is necessary to determine the ICE speed ω_{ice} in order to find the solution to Eqs. (20) and (21). In (Becerra *et al.*, 2011) ω_{ice} is found using information given by the ICE manufacturer. This information is not always available, instead efficiency maps, presented as a table, are used by most simulation tools (Markel *et al.*, 2002; Gao *et al.*, 2007).

Given a table ICE_{map} that maps ω_{ice} and τ_{ice} with an ICE efficiency, $ICE_{eff}(\omega_{ice}, \tau_{ice})$, the following algorithm can be applied:

1) Start with the lowest P_{ice}, minimum ω_{ice} and τ_{ice}, in the table ICE_{map}, and take it as base power P_{base}, and its corresponding ω_{base} and τ_{base}, for the first iteration.
2) Search on ICE_{map} the biggest neighbor to P_{base} (by increasing ω_{base} or τ_{base}) that offers the highest $\Delta ICE_{eff}/\Delta P_{ice}$ with respect to P_{base}.
The size of the search depends on the ICE and on the map, but it should be performed in neighbors around a 10% of the maximum power.
3) Add the power found in step 2, and its corresponding speed, to the table $\omega_{ice-eff}$.
4) Take as the new P_{base} the power found in step 2, and its corresponding ω_{base} and τ_{base}.
5) Repeat from step 2 until the maximum power from table ICE_{map} is reached.
6) The table generated in step 3 maps a given power to its most efficient speed, in other words, it generates $\omega_{ice-eff}(P_{ice})$.

Fig. 15 shows the plot of P_{ice} vs ICE_{eff} at a constant speed for the speeds defined in ICE_{map}. The upper contour is the plot of the table $\omega_{ice-eff}(P_{ice})$ found with the previous algorithm for the ICE that was chosen for simulations on this work. The plot of P_{ice} vs $\omega_{ice-eff}(P_{ice})$ is shown in Fig. 16.

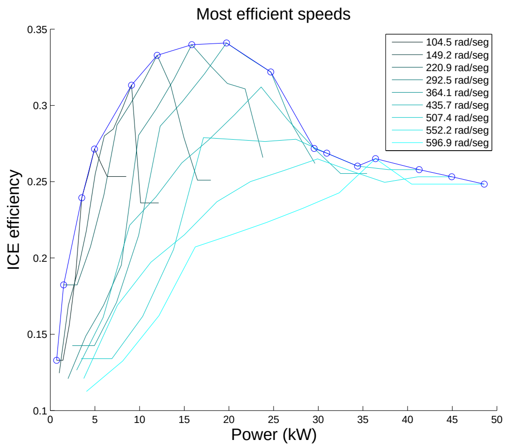

Fig. 15. ICE power vs efficiency at constant speed.

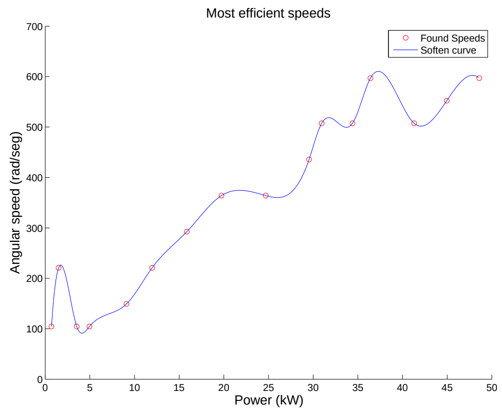

Fig. 16. ICE power vs efficient speed.

ACKNOWLEDGMENT

Research was supported by CONACYT 103640 and UNAM-PAPIIT IN105512 grants.

REFERENCES

Becerra, Guillermo, José Luis Mendoza-Soto and Luis Alvarez-Icaza (2011). Power flow control in hybrid electric vehicles. *ASME Conference Proceedings* **2011**(54761), 255–262.

Borhan, H.A., A. Vahidi, A.M. Phillips, M.L. Kuang and I.V. Kolmanovsky (2009). Predictive energy management of a power-split hybrid electric vehicle. In: *American Control Conference, 2009. ACC '09.*. pp. 3970 –3976.

Delprat, S., T.M. Guerra, G. Paganelli, J. Lauber and M. Delhom (2001). Control strategy optimization for an hybrid parallel powertrain. In: *American Control Conference, 2001. Proceedings of the 2001*. Vol. 2. pp. 1315 –1320.

Delprat, Sebastien, Jimmy Lauber, Thierry Marie Guerra and J. Rimaux (2004). Control af a parallel hybrid powertrain: optimal control. *IEEE Transactions on Vehicular Technology* **53**(3), 872–881.

Gao, D.W., C. Mi and A. Emadi (2007). Modeling and simulation of electric and hybrid vehicles. *Proceedings of the IEEE* **95**(4), 729 –745.

Gong, Qiuming, Yaoyu Li and Zhong-Ren Peng (2008). Trip-based optimal power management of plug-in hybrid electric vehicles. *Vehicular Technology, IEEE Transactions on* **57**(6), 3393 –3401.

Johannesson, Lars and Bo Egardt (2008). Approximate dynamic programming applied to parallel hybrid powertrains. In: *Proceedings of the 17th IFAC World Congress*. Vol. 17.

Kessels, John T. B. A., Michiel W. T. Koot, Paul P. J. van den Bosch and Daniel B. Kok (2008). Online energy management for hybrid electric vehicles. *Vehicular Technology, IEEE Transactions on* **57**(6), 3428 –3440.

Langari, R. and Jong-Seob Won (2003). Integrated drive cycle analysis for fuzzy logic based energy management in hybrid vehicles. In: *Fuzzy Systems, 2003. FUZZ '03. The 12th IEEE International Conference on*. Vol. 1. pp. 290 – 295.

Lin, Chan-Chiao, Huei Peng, J.W. Grizzle and Jun-Mo Kang (2003). Power management strategy for a parallel hybrid electric truck. *Control Systems Technology, IEEE Transactions on* **11**(6), 839 – 849.

Lin, Chan-Chiao, Huei Peng, Soonil Jeon and Jang Moo Lee (2002). Control of a hybrid electric truck based on driving pattern recognition. In: *Proceedings of the 2002 Advanced Vehicle Control Conference*.

Markel, T, A Brooker, T Hendricks, V Johnson, K Kelly, B Kramer, M OKeefe, S Sprik and K Wipke (2002). Advisor: a systems analysis tool for advanced vehicle modeling. *Journal of Power Sources* **110**(2), 255 – 266.

Musardo, C., G. Rizzoni and B. Staccia (2005). A-ecms: An adaptive algorithm for hybrid electric vehicle energy management. In: *Decision and Control, 2005 and 2005 European Control Conference. CDC-ECC '05. 44th IEEE Conference on*. pp. 1816 – 1823.

Schouten, Niels J., Mutasim A. Salman and Naim A. Kheir (2002). Fuzzy logic control for parallel hybrid vehicles. *IEEE Transactions on Vehicular Technology* **Vol. 10**, 460–468.

Sciarretta, A. and L. Guzzella (2007). Control of hybrid electric vehicles. *Control Systems, IEEE* **27**(2), 60 –70.

Sciarretta, A., M. Back and L. Guzzella (2004). Optimal control of parallel hybrid electric vehicles. *Control Systems Technology, IEEE Transactions on* **12**(3), 352 – 363.

van Keulen, T., B. de Jager, A. Serrarens and M. Steinbuch (2010). Optimal energy management in hybrid electric trucks using route information. *Oil & Gas Science and Technology* **65**(1), 103–113.

Zhang, Chen, Ardalan Vahidi, Pierluigi Pisu, Xiaopeng Li and Keith Tennant (2010). Role of terrain preview in energy management of hybrid electric vehicles. *IEEE Trans. Veh. Technol* **59**(3), 1139–1147.

Zhang, Xiangqun, Jack Katzberg, Bruce Cooke and J.Kos (1997). Modeling and simulation of a hybrid-engine. *Conference on Communications, Power and Computing, Winnipeg, MB* pp. 286–291.